Electronic Supplementary Material (ESI) for Chemical Science.

Electronic Supporting Information
Regioselectivity of Concerted Proton-Electron Transfer at the Surface of a Polyoxovanadate Cluster

Eric Schreiber, William W. Brennessel, and Ellen M. Matson*
Department of Chemistry, University of Rochester, Rochester NY, USA 14627

Supporting Information Table of Contents:

Table S1. Crystallographic parameters of the molecular structures obtained for complexes **2-$V_6O_8^{2-}$** and **3-$V_6O_7(OH)^{2-}$**

Compound	**2-$V_6O_8^{2-}$**	**3-$V_6O_7(OH)^{2-}$**
Empirical formula	$C_{31}H_{53}O_{19}Co_2V_6$	$C_{43}H_{106}N_2O_{19}V_6$
Formula weight	1153.23	1260.93
Temperature / K	223.00(10)	100.00(10)
Wavelength / Å	1.54184	1.54184
Crystal group	Orthorhombic	Triclinic
Space group	*Pnna*	*P-1*
Unit cell dimensions	a = 16.8845(2) Å b = 41.3260(6) Å c = 14.1744(3) Å α = 90° β = 90° γ = 90°	a = 11.98260(10) Å b = 11.99650(10) Å c = 13.43130(10) Å α = 95.1060(10)° β = 115.5700(10)° γ = 113.8640(10)°
Volume / Å^3	9890.5(3)	1509.23(3)
Z	8	1
Reflections collected	124947	95852
Independent reflections	67691	51188
Completeness (theta)	100.0% (74.504°)	99.7% (74.504°)
Goodness-of-fit on F^2	1.064	1.078
Final R indices [I>2sigma(I)]	$R1$ = 0.0854	$R1$ = 0.0361
Largest diff. peak and hole	2.392 and -1.301 e.Å^{-3}	1.082 and -1.015 e.Å^{-3}

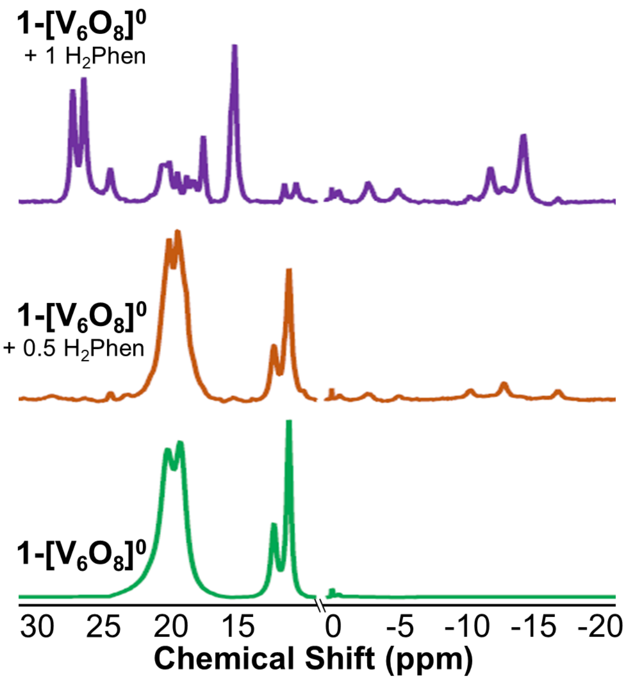

Figure S1. ^1H NMR spectra of $\mathbf{1\text{-}V_6O_8{}^0}$ and reactions with ½ and 1 equiv of H_2Phen at 21°C in CD_3CN.

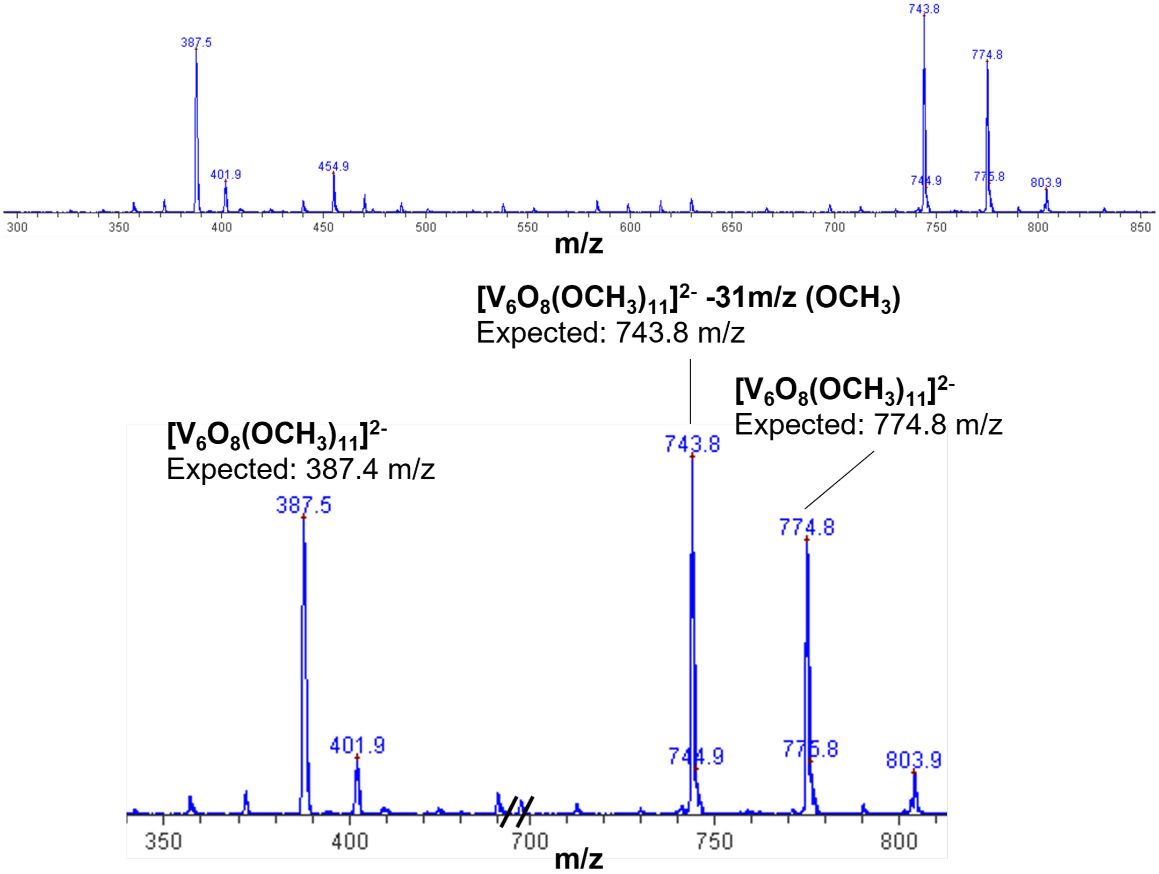

Figure S2. ESI-MS of $\mathbf{2\text{-}V_6O_8{}^{2-}}$.

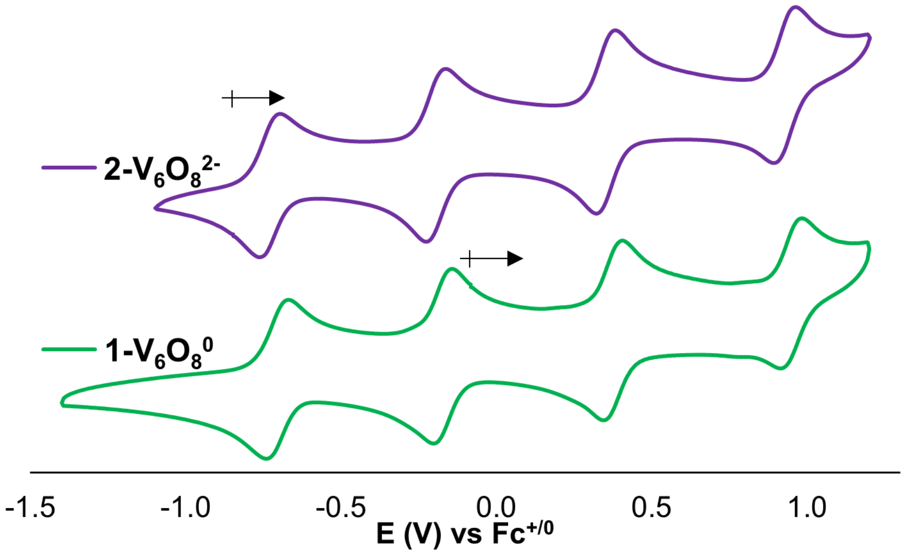

Figure S3. Cyclic voltammogram of 1 mM **1-$V_6O_8^0$** (green, bottom) and **2-$V_6O_8^{2-}$** (purple, top) collected in MeCN with 100 mM [$^nBu_4N$][PF_6] supporting electrolyte at 100 mV/s.

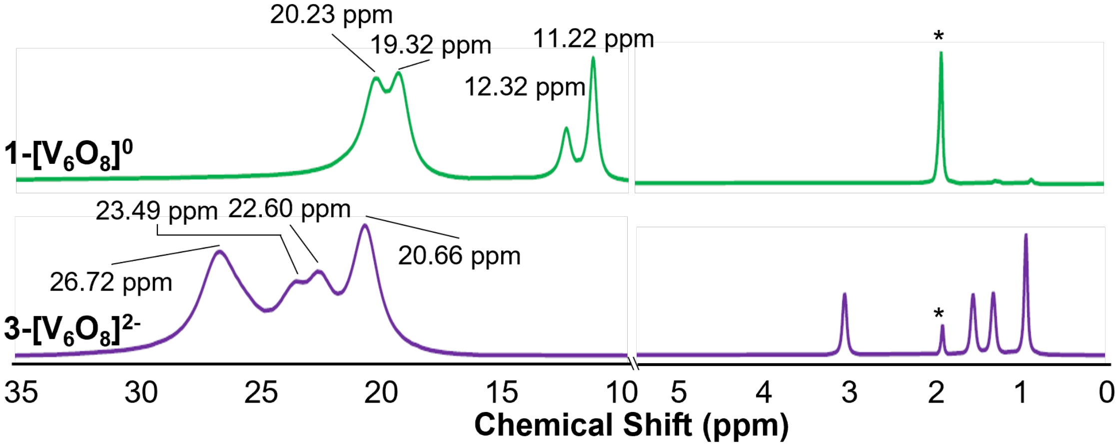

Figure S4. ^1H NMR spectra of **1-$V_6O_8^0$** and **2-$V_6O_8^{2-}$** at 21°C in CD_3CN.

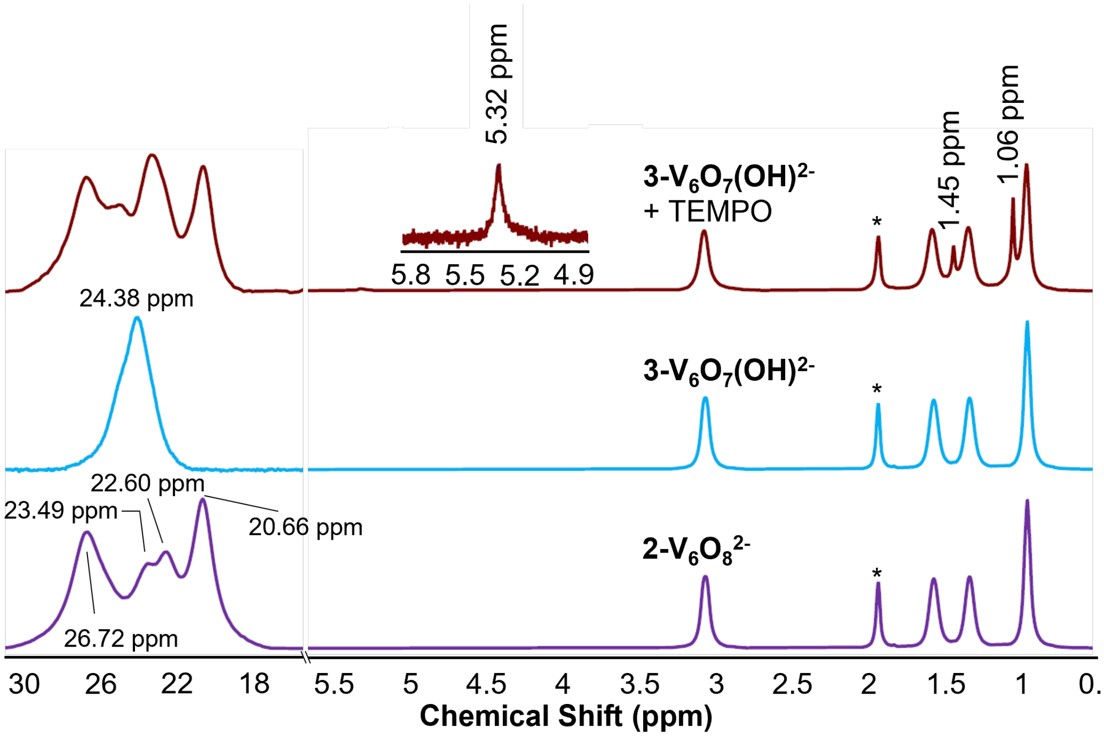

Figure S5. ^{1}H NMR spectra of **2-$V_6O_8^{2-}$** (purple, bottom), **3-$V_6O_7(OH)^{2-}$** (teal, middle), and **3-$V_6O_7(OH)^{2-}$** after reacting with 1 equivalent of TEMPO (red, top) recorded in CD_3CN at 21°C.

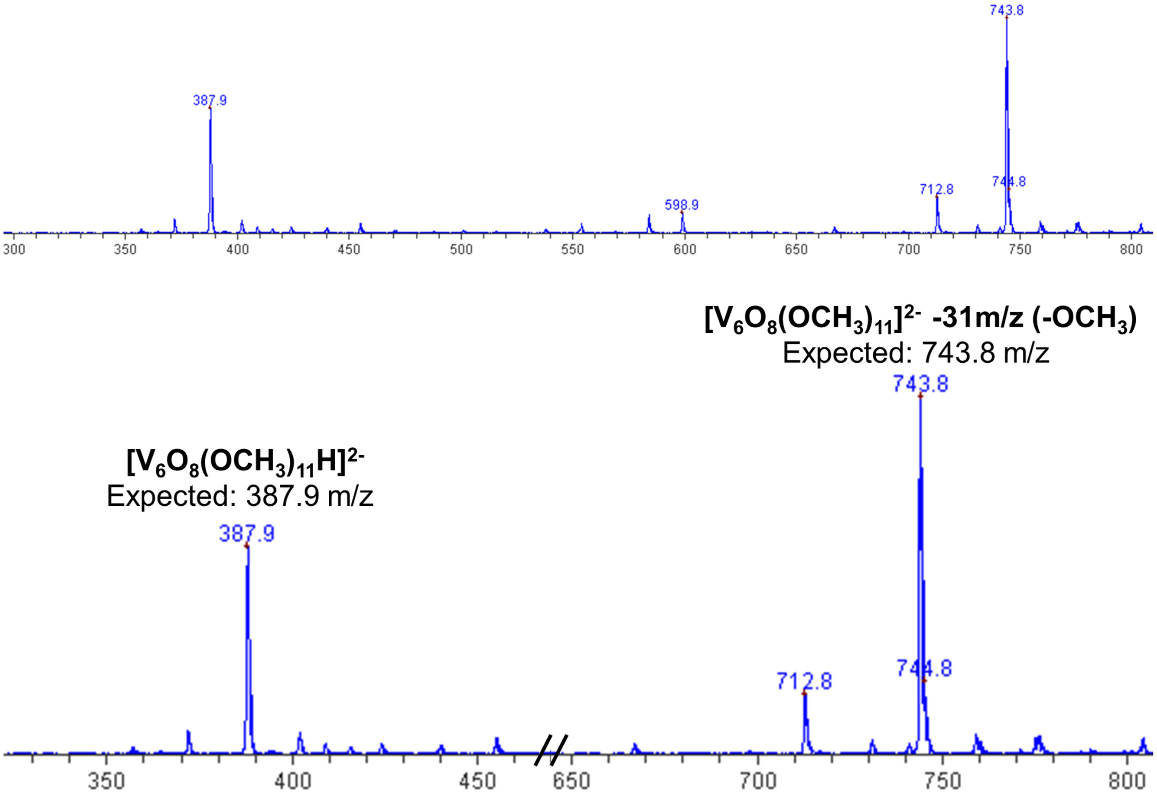

Figure S6. ESI-MS of **3-$V_6O_7(OH)^{2-}$**.

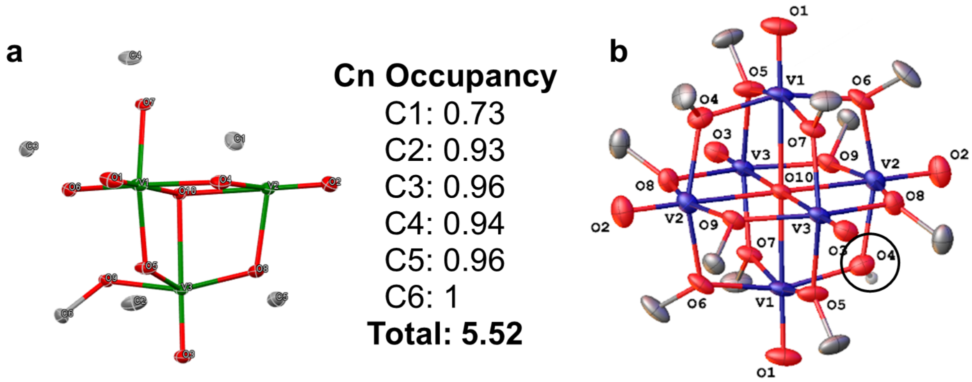

Figure S7. Single crystal X-ray structure of **$3\text{-}V_6O_7(OH)^{2-}$**. a) Cluster asymmetric unit with C-atom occupancies. b) Cluster formula unit after data refinement, with the O4-H bond highlighted.

Table S2. Bond valence sum calculations on X-ray crystal structure data of **$2\text{-}V_6O_8^{2-}$**. Bolded values indicate the representative oxidation state of the respective ion.

Complex	Oxidation State (V^n)	V1[a]	V2[a]	V3	V4	V5	V6
$3\text{-}V_6O_8(OCH_3)_{11}^{2-}$	V^{IV}	4.490	**4.023**	**4.071**	**4.044**	**4.024**	**3.999**
	V^{V}	**4.779**	4.291	4.340	4.314	4.292	4.266

[a] Indicates V ions bound to the μ_2-oxide.

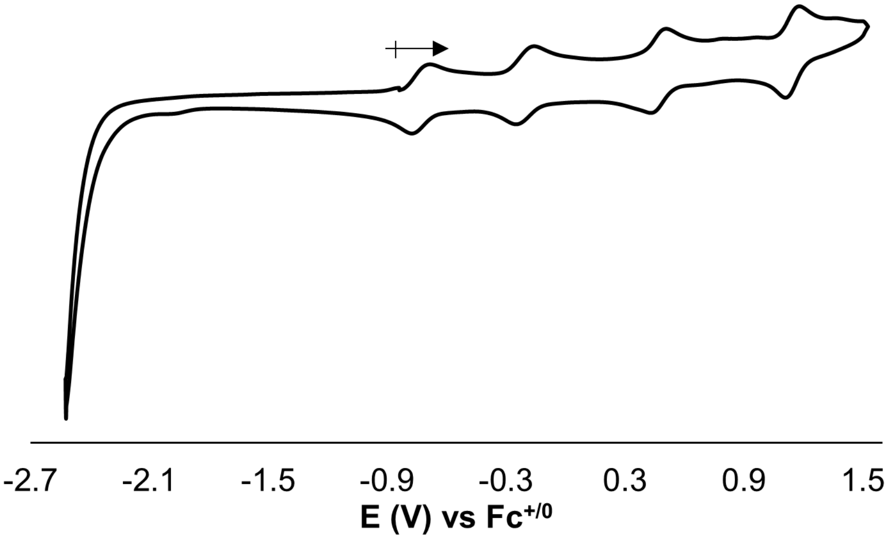

Figure S8. Cyclic voltammogram of 1 mM **$2\text{-}V_6O_8^{2-}$** from 1.5 to -2.5 V vs $Fc^{+/0}$ collected in MeCN with 100 mM [$^nBu_4N$][PF_6] supporting electrolyte at 100 mV/s.

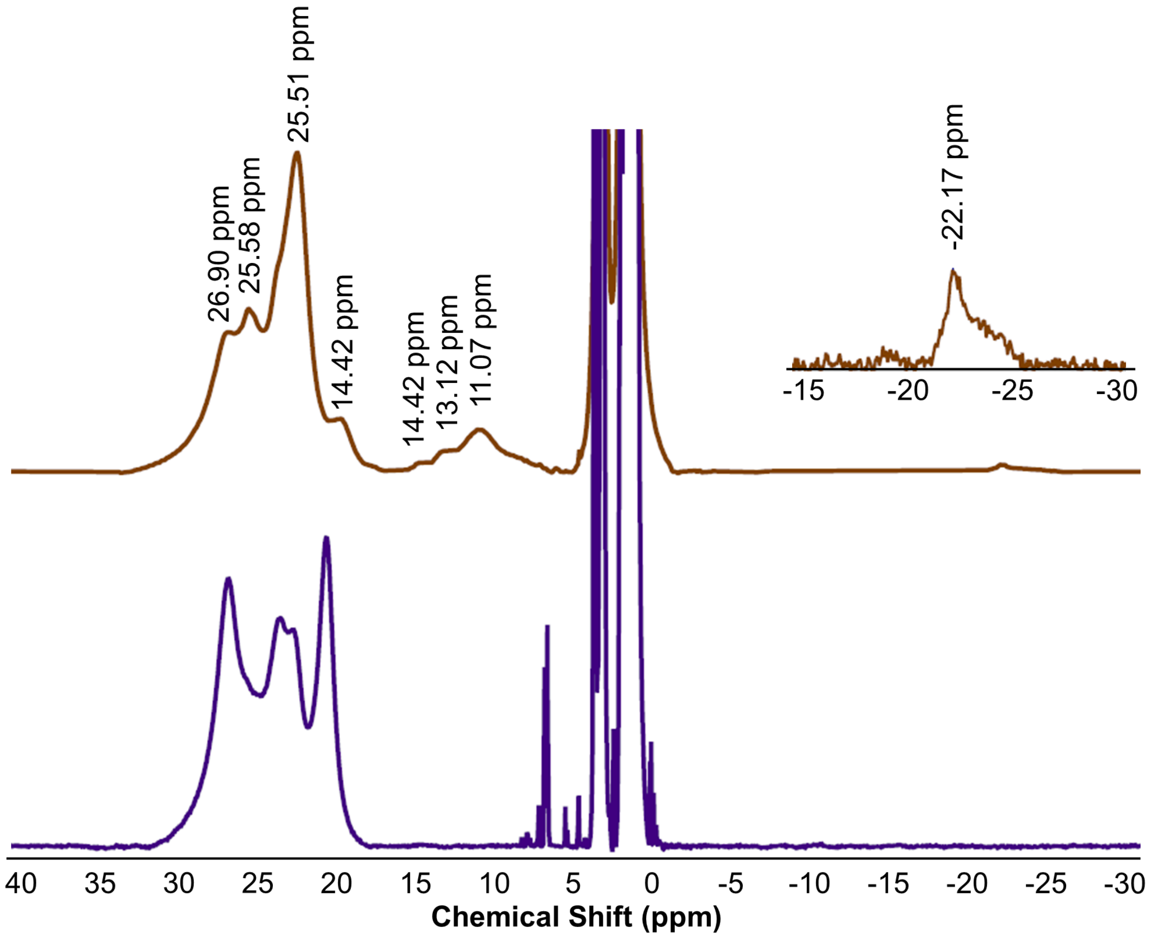

Figure S9. ^{1}H NMR spectra of **2-V$_6$O$_8$$^{2-}$** before (purple, bottom), and after exposure to one equivalent of triethylammonium tetrafluoroborate (brown, top) recorded in CD$_3$CN at 21°C.

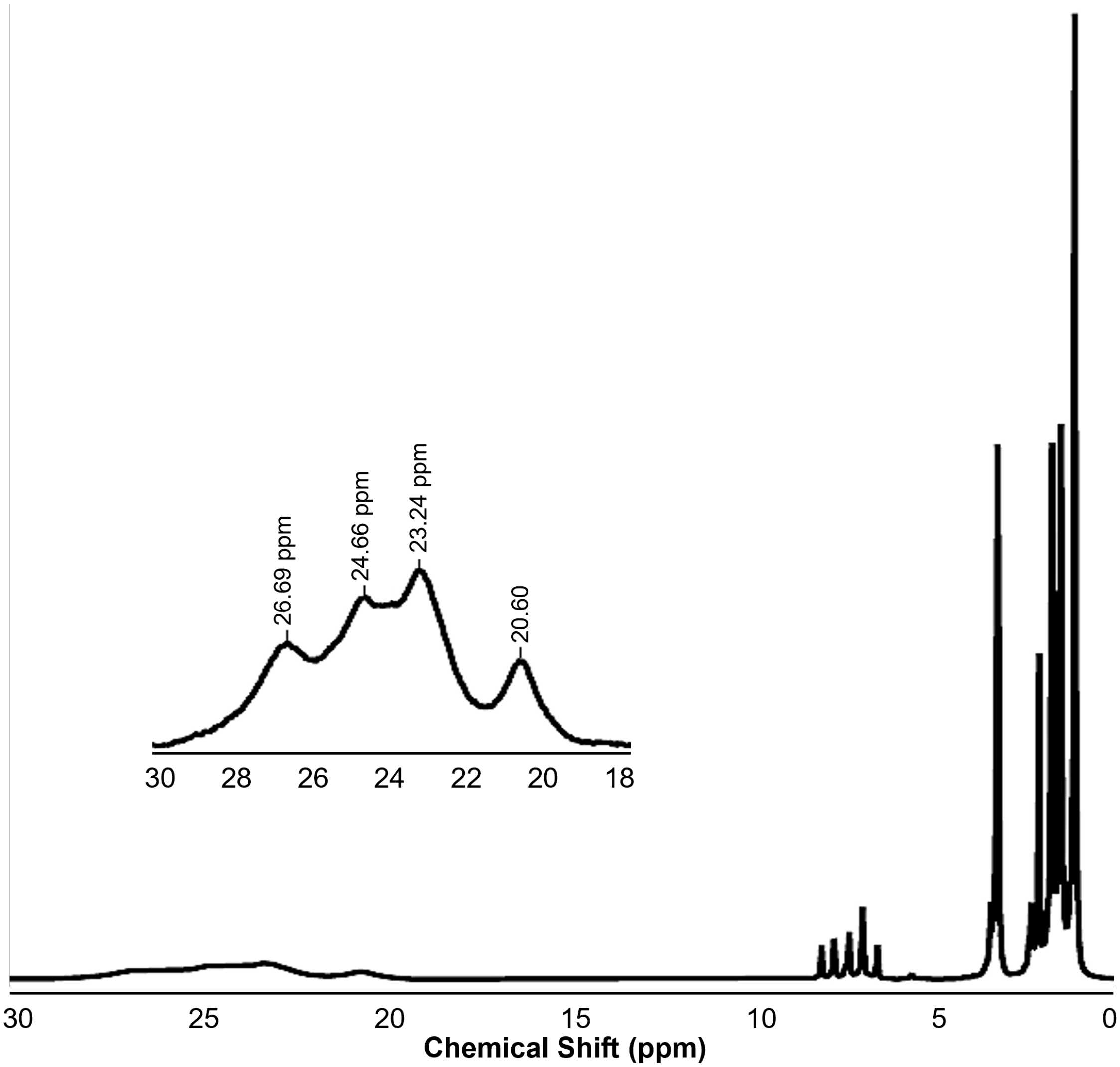

Figure S10. Paramagnetic region of the ^{1}H NMR spectrum of **2-$V_6O_8^{2-}$** after exposure to half an equivalent of hydrazobenzene at 21°C for 14 days recorded in CD_3CN at 21°C.

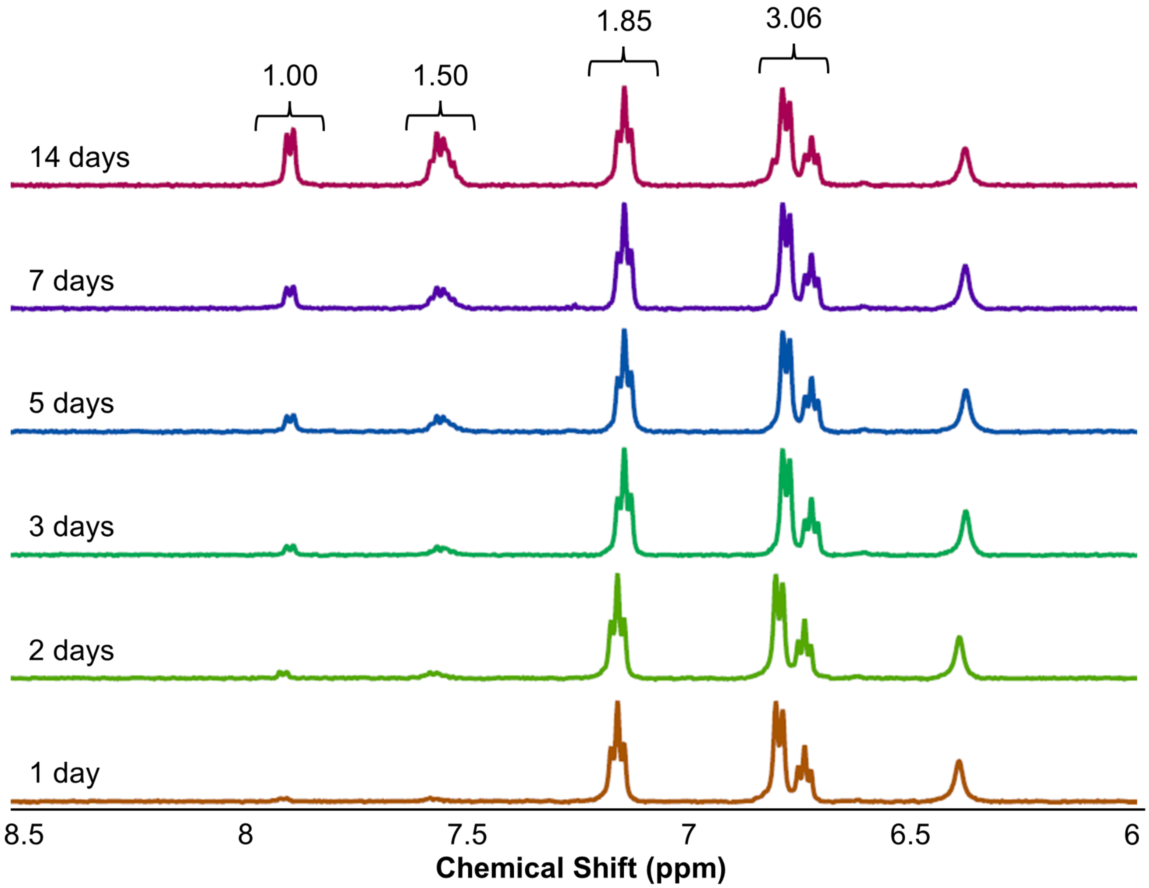

Figure S11. ^{1}H NMR spectra of hydrazobenzene after exposure to two equivalents of $\mathbf{2\text{-}V_6O_8^{2-}}$ at 21°C for 14 days recorded in CD_3CN at 21°C (Trial A).

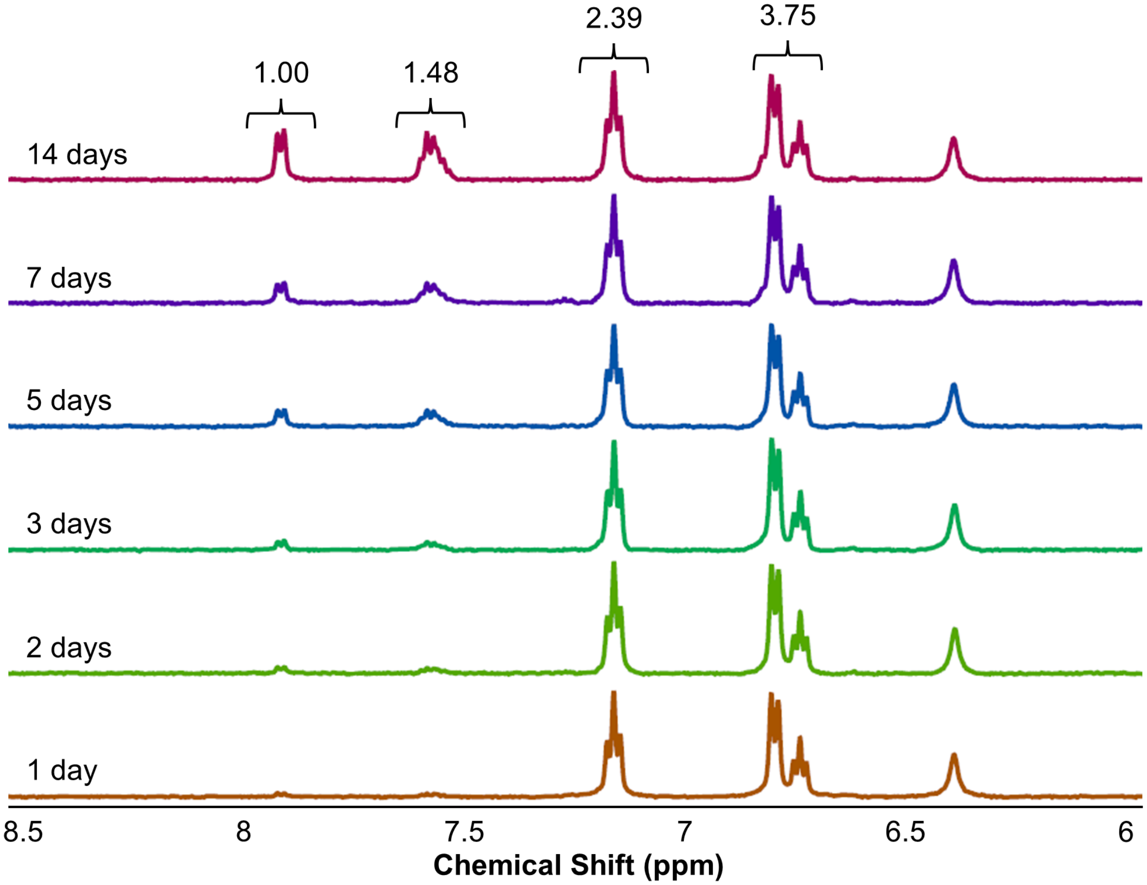

Figure S12. ^{1}H NMR spectra of hydrazobenzene after exposure to two equivalents of $\mathbf{2\text{-}V_6O_8}^{2-}$ at 21°C for 14 days recorded in CD_3CN at 21°C (Trial B).

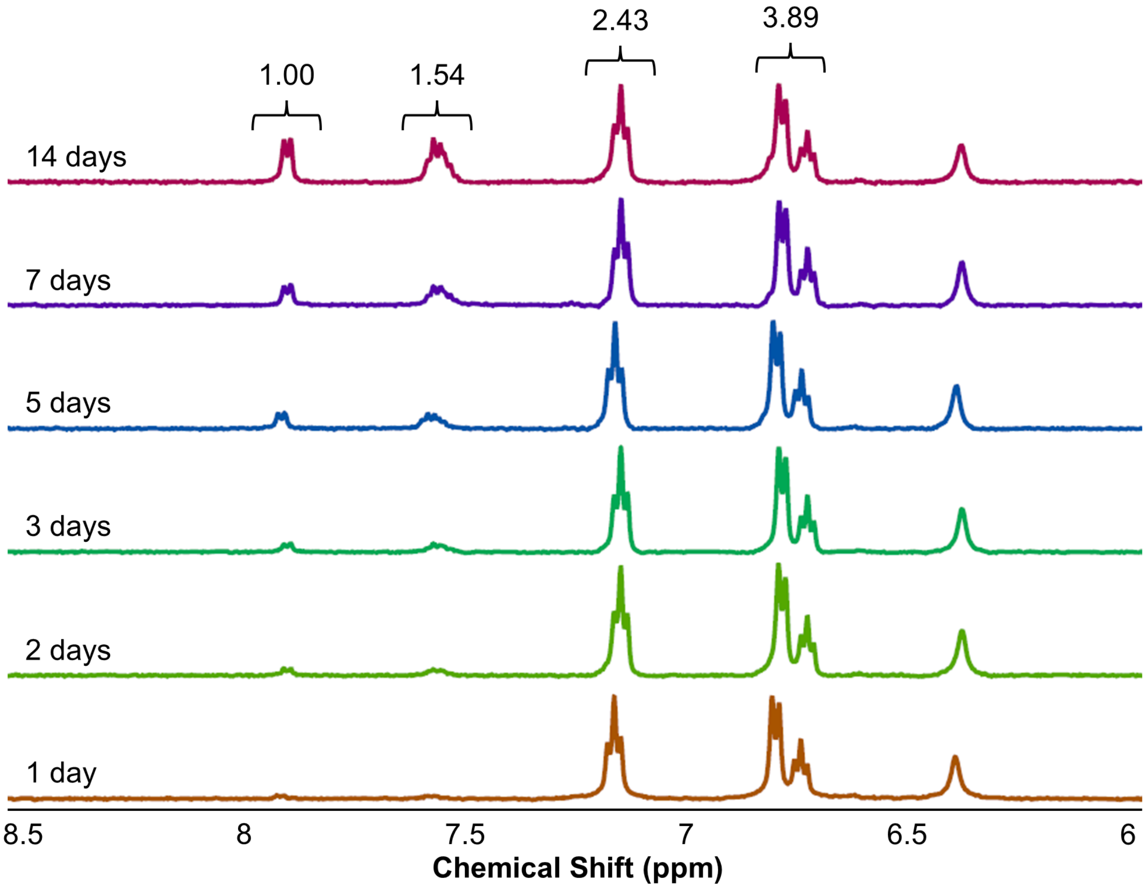

Figure S13. ^{1}H NMR spectra of hydrazobenzene after exposure to two equivalents of **$2\text{-}V_6O_8^{2-}$** at 21°C for 14 days recorded in CD_3CN at 21°C (Trial C).

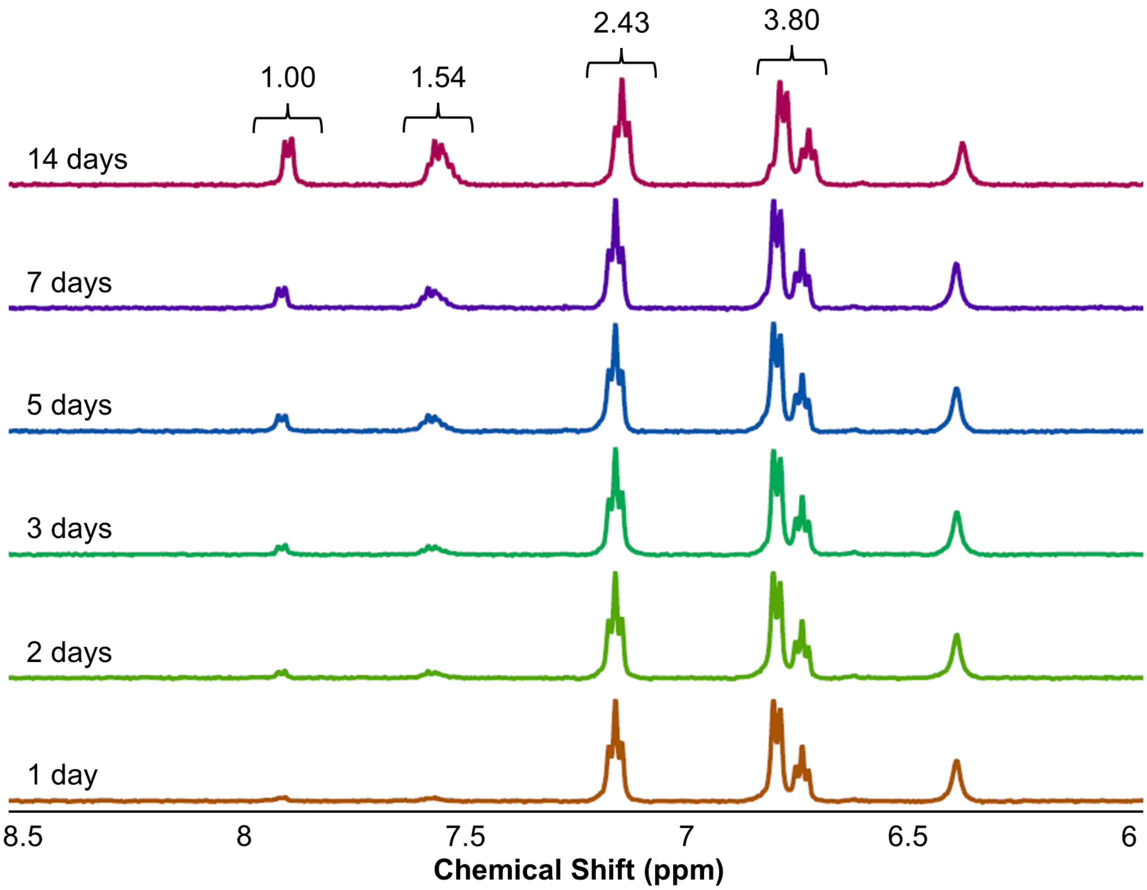

Figure S14. ^{1}H NMR spectra of hydrazobenzene after exposure to two equivalents of **$2\text{-}V_6O_8^{2-}$** at 21°C for 14 days recorded in CD_3CN at 21°C (Trial D).

Table S3. $BDFE_{adj}$ calculated from equilibrated reactions between **$2\text{-}V_6O_8^{2-}$** and half an equivalent of Hydz described in Figure S8, using the equation for $BDFE_{adj}$.

	Hydrazobenzene[b]					**Azobenzene**					
	7.16 ppm (4 H)		**6.77 ppm (6 H)**		**Avg. Conc.**	**7.91 ppm (4 H)**		**7.58 ppm (6 H)**		**Avg. Conc.**	**$BDFE_{adj}$ (kcal/mol)**
Trial	Integral	Relative Conc.[a]	Integral	Relative Conc.[a]		Integral	Relative Conc.[a]	Integral	Relative Conc.[a]		
A	1.85	0.463	3.06	0.510	**0.486**	1.00	0.250	1.50	0.250	**0.250**	**60.7**
B	2.39	0.598	3.75	0.625	**0.611**	1.00	0.250	1.48	0.247	**0.248**	**60.6**
C	2.43	0.608	3.89	0.648	**0.628**	1.00	0.250	1.54	0.257	**0.253**	**60.6**
D	2.43	0.608	3.80	0.633	**0.620**	1.00	0.250	1.54	0.257	**0.253**	**60.6**
										Avg.	**60.6**
										Std. Dev.	**0.1**

[a] Relative concentration of either hydrazobenzene or azobenzene was determined by dividing the integral by the number of protons a given signal(s) corresponds with.

[b] Integration of the N-H resonance of hydrazobenzene was omitted in this study due to potential broadening of the resonance by H-bonding with **$2\text{-}V_6O_8^{2-}$**.

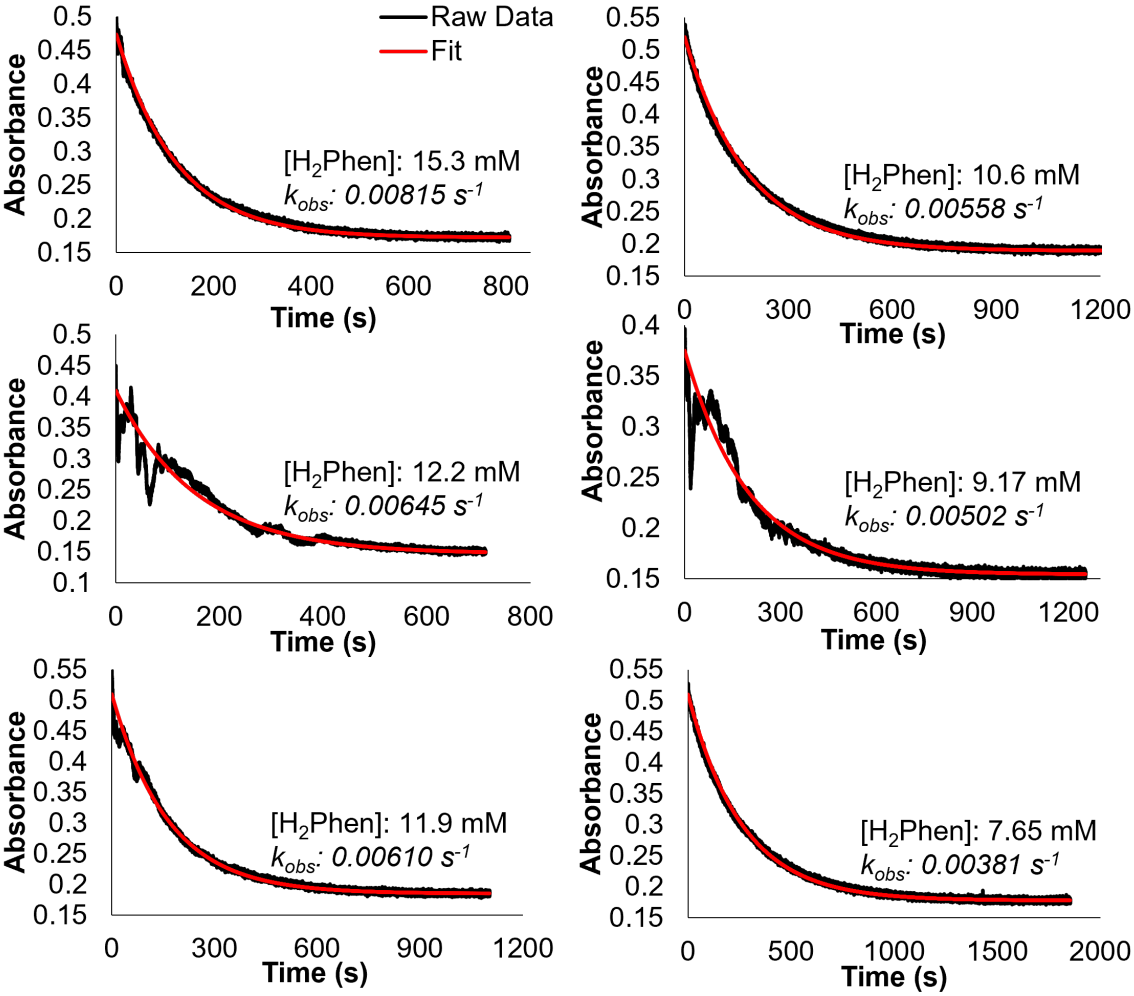

Figure S15. Plots of absorbance at 1024 nm over time for reactions between **2-$V_6O_8^{2-}$** (1.45 mM) and excess H_2Phen under pseudo-first order conditions recorded in CH_3CN at -25 °C, with raw data (black curve) fit by the equation defined in the relevant portion of the Experimental section (red curve). Concentration of H_2Phen for each reaction is noted, alongside the fit-derived k_{obs}.

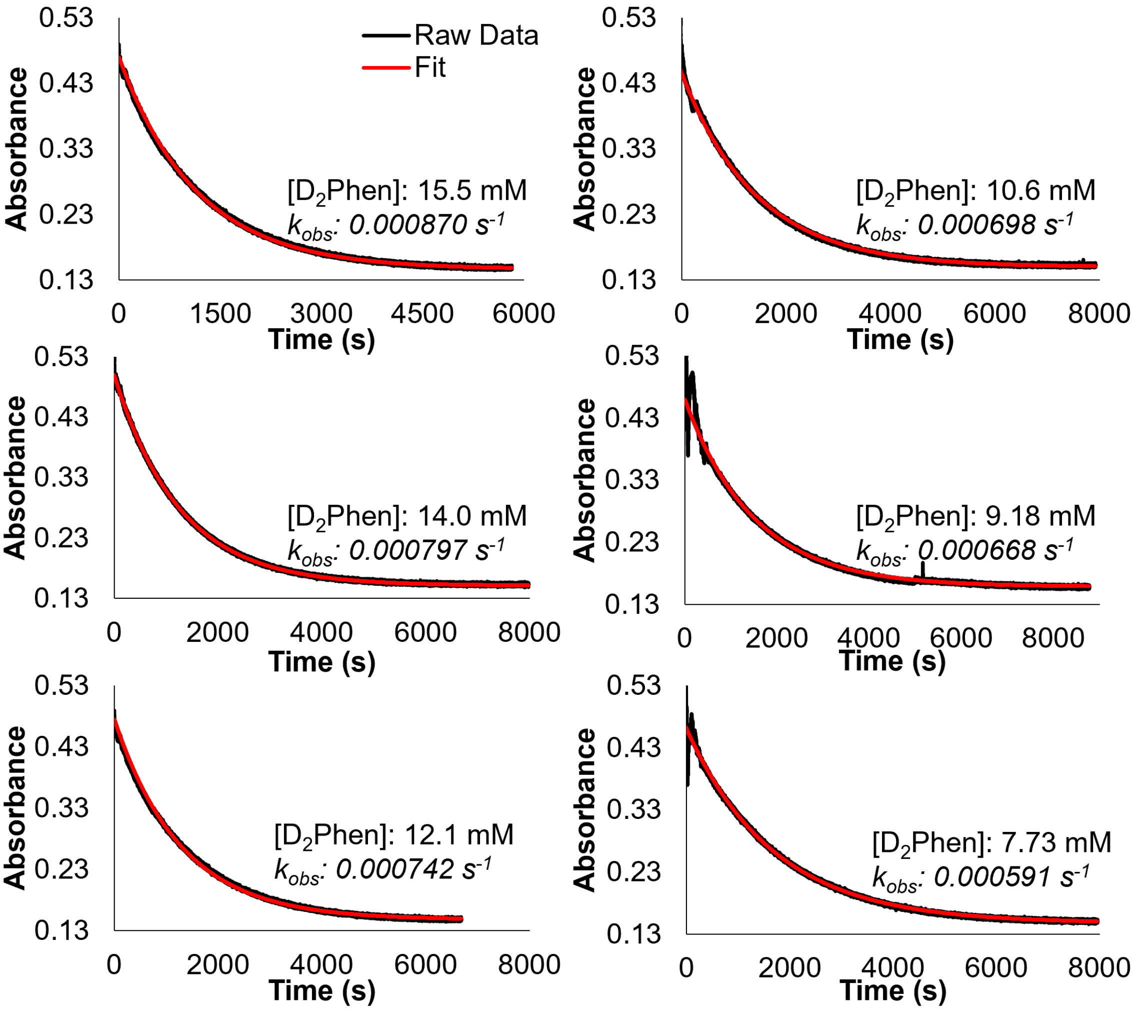

Figure S16. Plots of absorbance at 1024 nm over time for reactions between **2-$V_6O_8^{2-}$** (1.45 mM) and excess D_2Phen under pseudo-first order conditions recorded in CH_3CN at -25 °C, with raw data (black curve) fit by the equation defined in the relevant portion of the Experimental section (red curve). Concentration of D_2Phen for each reaction is noted, alongside the fit-derived k_{obs}.

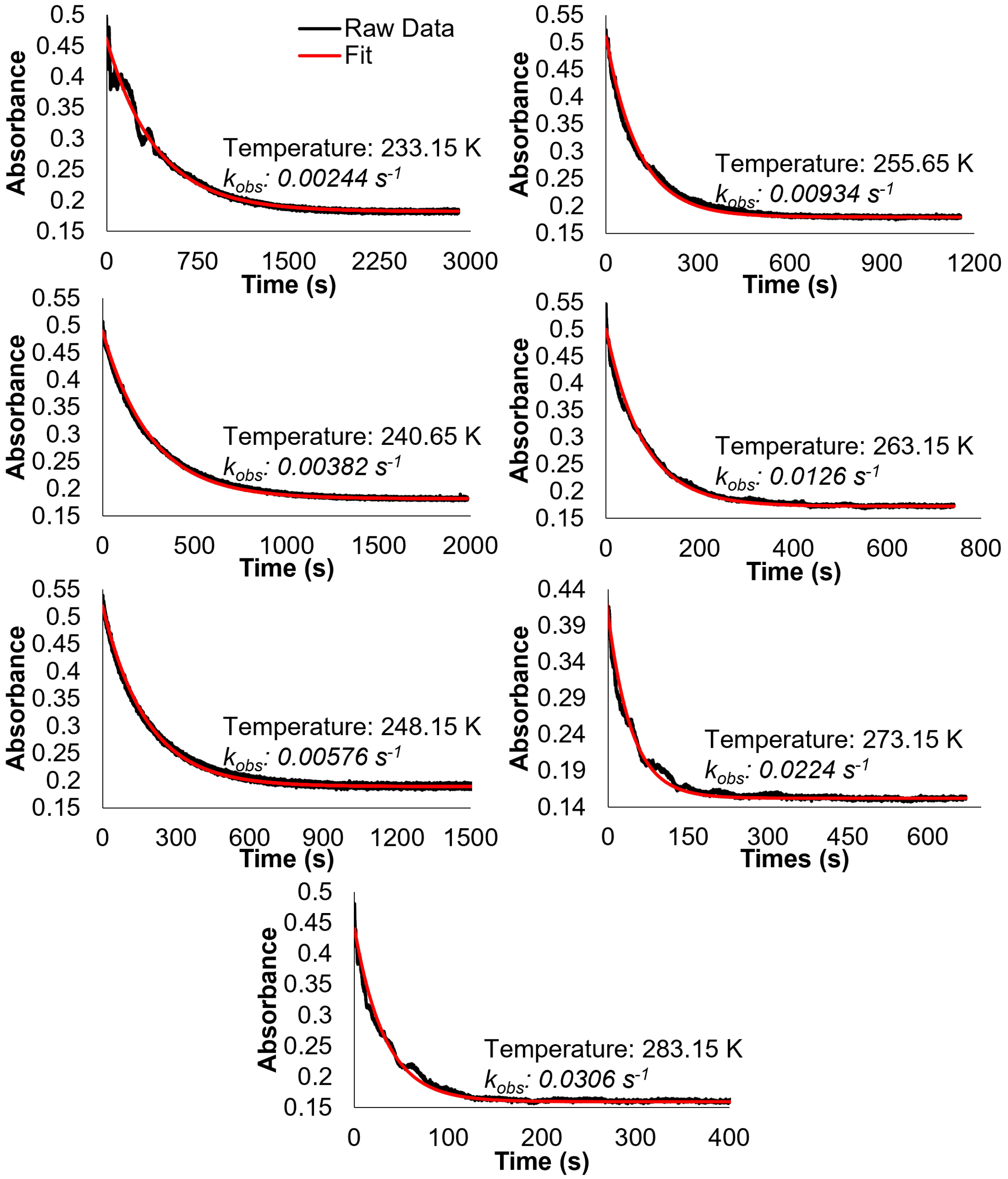

Figure S17. Plots of absorbance at 1024 nm over time for reactions between $\mathbf{2\text{-}V_6O_8^{2-}}$ (1.45 mM) and H_2Phen (10.6 mM) recorded in CH_3CN between -40 and 10 °C, with raw data (black curve) fit by the equation defined in the relevant portion of the Experimental section (red curve), providing k_{obs} and k_{exp} (after dividing by the concentration of H_2Phen).

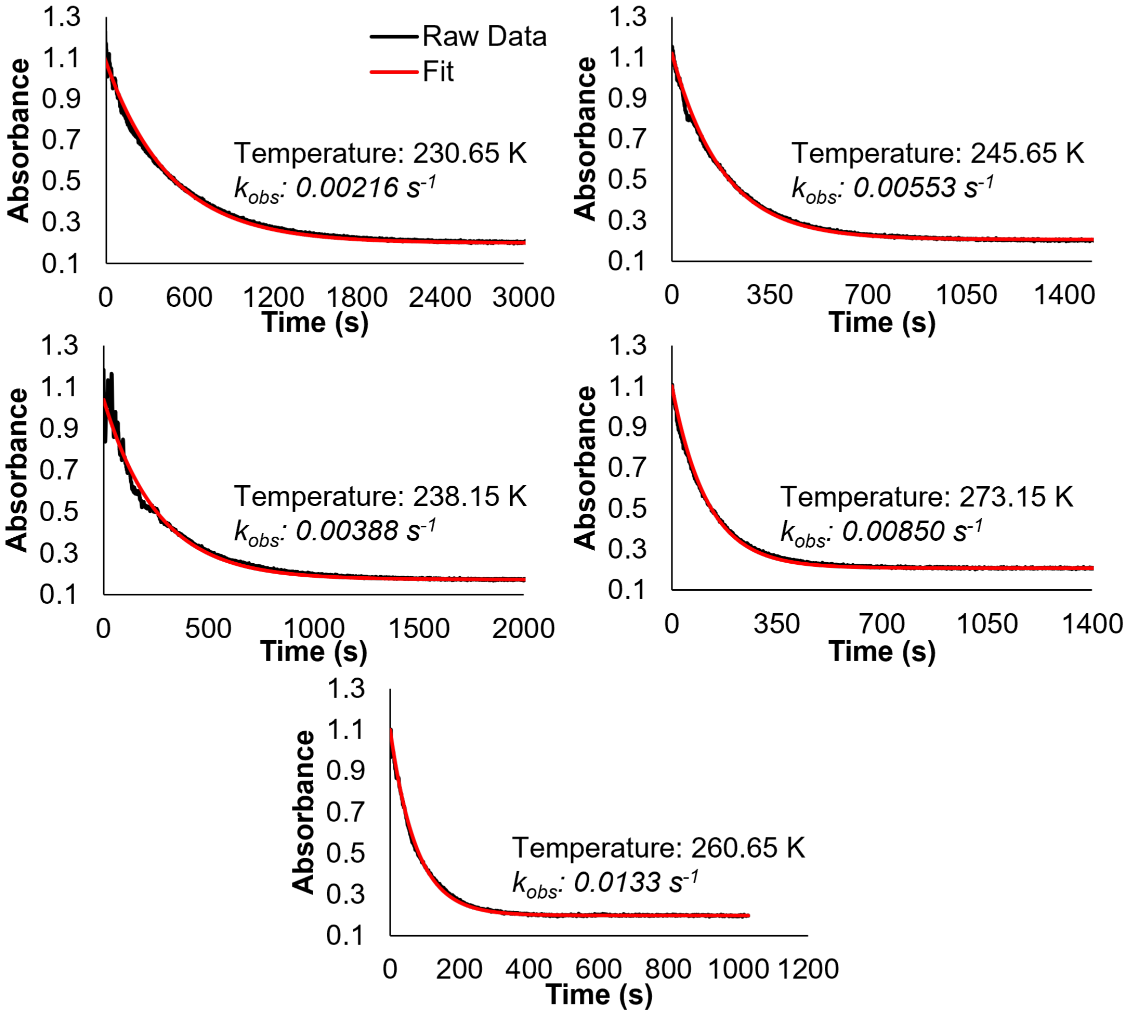

Figure S18. Plots of absorbance at 1050 nm over time for reactions between [$^{n}Bu_4N$][$V_6O_7(OCH_3)_{12}$] (1.44 mM) with H_2Phen (16.44 mM) recorded in CH_3CN between -42.5 and –12.5 °C, with raw data (black) and a fit curve (red), providing k_{obs} and k_{exp}.

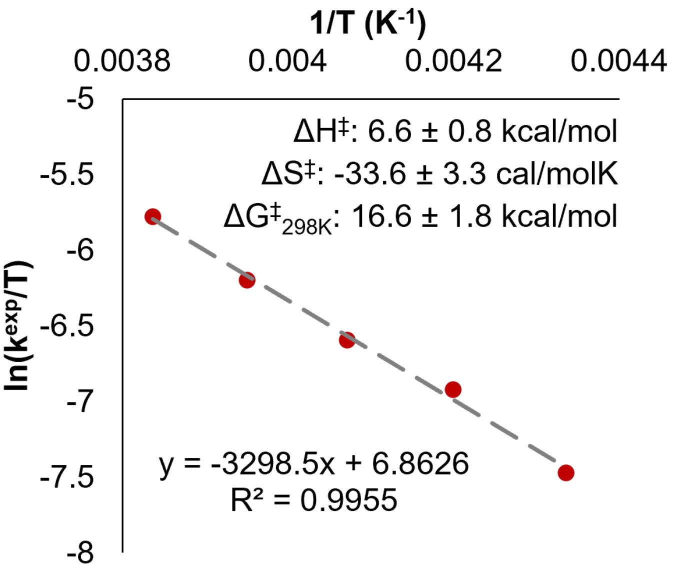

Figure S19. Eyring plot for the reaction of [^{n}Bu$_4$N][$V_6O_7(OCH_3)_{12}$] (1.44 mM) with H_2Phen (16.44 mM) in CH_3CN between -42.5 and -12.5 °C. Y-axis values were determined by dividing k_{obs} by the concentration of H_2Phen, providing the rate constant, k_{exp}. Activation parameters are labelled on the plot.

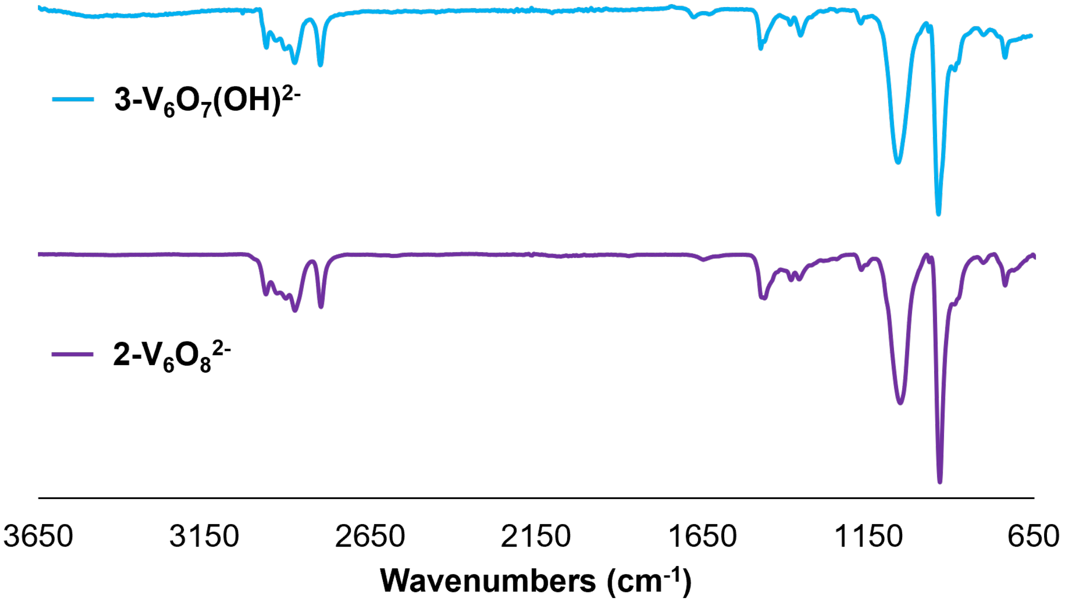

Figure S18. FTIR (ATR) spectrum of **2-$V_6O_8^{2-}$** and **3-$V_6O_7(OH)^{2-}$**.